DOA Refinement through Complex Parabolic Interpolation of a Sparse Recovered Signal

Luca Pallotta, *Senior Member, IEEE,* Gaetano Giunta, *Senior Member, IEEE* and Alfonso Farina, *Life Fellow, IEEE*

***Abstract*—This letter considers the design of a two-stage direction of arrival (DOA) scheme for radar systems. Precisely, at the first stage a sparse recovery approach is used to obtain both DOA and complex amplitude estimates of the incoming signal. Since the DOA is evaluated on a predefined grid of bins sampling the antenna azimuth mainbeam, at the second stage, a closed-form complex-valued parabolic interpolation is performed to refine it. By doing so, the angle accuracy is improved, but at the same time maintaining fixed the overall computational complexity. Numerical results show the enhancement provided by the proposed procedure to the initial sparse recovery method.**

***Index Terms*—DOA estimation, radar, complex-valued parabolic interpolation, sparse recovery.**

I. Introduction

Direction of arrival (DOA) estimation of an incoming signal is one of key-operation in modern receiving systems. As a matter of fact, several methodologies have been developed during the years to properly solve this important issue that spans a wide family of applications in the context of signal processing, viz. from radar to sonar, to wireless communications, etc. This so wide interest has driven many researches in developing algorithms capable of accurately estimating the DOA of the signal impinging on the receiving antenna. Among them, of paramount importance are the classic Capon [1], ESPRIT [2], MUSIC, as well as the plethora of works extending them and that, in general, exploits several kinds of advanced statistical and signal processing techniques [3]–[11]. Additionally, several procedures for DOA estimation exploiting the sparse nature of the signal model associated with targets/signals in number less than possible sources angle of arrivals (AOAs) in the region of interest have been devised [12]–[16]. Within this latter category, the sparse learning via iterative minimization (SLIM) developed in [12] consists in a regularized minimization algorithm that also applies an l_q-norm constraint to obtain an accurate estimate of the signal angle, range, and Doppler. Moreover, SLIM is characterized by a capability of offering satisfactorily estimation performance with a relatively low computational burden.

In this letter, we devise a two-stage procedure aimed at improving the angle estimation accuracy of an incoming signal towards the radar receiving system. Precisely, following the lead of [12], as in [17], we first divide the observed azimuth angular region on a grid of equally-spaced bins including the antenna mainbeam. Then, we apply the SLIM procedure to have an estimate of the target AOA and amplitude. Starting from the AOA and complex amplitude estimated by the SLIM, the second step consists in using a complex-valued parabolic interpolating function derived through a Least Squares (LS) approach to refine the angle estimate. Remarkably, the second stage does not impact on the overall computational complexity of the procedure due to its closed-form expression. Several tests are conducted by simulations considering the proposed procedure with two different complex-valued interpolating functions also in comparison with their real counterpart and compared to the output given by the SLIM at the first stage. The results point out that the proposed procedure is capable of ensuring some accuracy improvements without increasing the computational cost directly related to the grid step size.

The letter is organized as follows. The problem is formalized in Section II. In Section III the sparse recovery procedure is described, whereas the complex parabolic interpolators for DOA refinement are detailed in Section IV. The effectiveness of the proposed procedure is demonstrated by simulations in Section V. Finally, Section VI concludes the letter together with some hints for future works.[1]

II. Problem formulation

A search radar with a uniform linear array (ULA) composed by N equally-spaced antenna elements is herein considered. The radar beampattern illuminates a specific angular region (say in azimuth) and acquires the signal scattered by different range cells[2]. Then, the radar elaborates the signal cell-by-cell to decide for the target presence as well as to estimate target velocity, DOA, and so on [4]. More specifically, the datum of the cell under test, say $\boldsymbol{r} \in \mathbb{C}^{N\times 1}$, is defined as

$$\boldsymbol{r} = \alpha \boldsymbol{s}(\theta_t) + \boldsymbol{i}, \tag{1}$$

[1] *Notation:* Boldface lower- and upper-case denote vectors and matrices, respectively. The symbols $(\cdot)^T$ and $(\cdot)^\dagger$ are the transpose and conjugate transpose. Moreover, $\mathbb{C}$ is the set of complex numbers and $\mathbb{C}^{N\times M}$ is the Euclidean space of $(N \times M)$-dimensional complex matrices (or vectors if $M = 1$). Given a vector $\boldsymbol{a}$, $\mathbf{diag}(\boldsymbol{a})$ indicates the diagonal matrix whose i-th diagonal element is the i-th entry of $\boldsymbol{a}$, whereas $\|\boldsymbol{a}\|$ is its Euclidean norm. For a random variable x, $x \sim \mathcal{U}[x_1, x_2]$ means that x is uniformly distributed in the interval $[x_1, x_2]$. Finally, $\Re\{\cdot\}$, $\Im\{\cdot\}$, and $|\cdot|$ indicate the real part, imaginary part and modulus of a complex number, respectively.

[2] It is worth recalling that in radar contexts the monopulse technique is widely used to perform angular measurement. The interested reader could refer to references [18]–[21] on this challenging method as well as its implementations in scenarios of practical interest.

L. Pallotta and G. Giunta are with Department of Engineering, University of Roma Tre, via Vito Volterra 62, 00146 Rome, Italy. E-mail: luca.pallotta@uniroma3.it, gaetano.giunta@uniroma3.it.

A. Farina, Selex ES (retired), is a Consultant, 00144 Rome, Italy. E-mail: alfonso.farina@outlook.it.

Copyright (c) 2021 IEEE. Personal use is permitted. For any other purposes, permission must be obtained from the IEEE by emailing pubs-permissions@ieee.org.

with $\boldsymbol{i} \in \mathbb{C}^{N\times 1}$ the interference term (possibly composed by clutter, jamming, and noise) modeled as a zero-mean complex Gaussian random vector with unknown covariance matrix $\boldsymbol{M} \in \mathbb{C}^{N\times N}$, α the complex amplitude accounting from channel propagation effects, target reflectivity, and antenna beampattern shape. Moreover, θ_t is the AOA of the target (typically assumed equal to the antenna pointing direction), and $\boldsymbol{s}(\theta) = [1, \exp\{j\pi\sin(\theta)\}, \ldots, \exp\{j(N-1)\pi\sin(\theta)\}]^T \in \mathbb{C}^{N\times 1}$ is the nominal steering vector, having set the separation between antenna's elements equal to one-half the radar operating wavelength.

Now, to properly estimate the DOA of the detected target, we first consider a method based upon a sparse recovery method. Then, we apply a specific quadratic interpolating function to refine this estimation. More precisely, as in [17], we divide the observed angular region in N_a azimuth bins separated by $\Delta\theta$ assuming the target returns contained in this specific region (including the antenna mainbeam). Therefore, indicating with θ_m, $m = 1, \ldots, N_a$, the m-th azimuth angle, the signal from the cell under test can be cast as

$$\boldsymbol{r} = \sum_{m=1}^{N_a} \alpha_m \boldsymbol{s}(\theta_m) + \boldsymbol{i} = \boldsymbol{S}\boldsymbol{\alpha} + \boldsymbol{i}, \tag{2}$$

with $\boldsymbol{S} = [\boldsymbol{s}(\theta_1), \cdots, \boldsymbol{s}(\theta_{N_a})] \in \mathbb{C}^{N\times N_a}$ the steering dictionary matrix and $\boldsymbol{\alpha} = [\alpha_1, \cdots, \alpha_{N_a}]^T \in \mathbb{C}^{N_a\times 1}$ the amplitude vector whose entries are the target responses. Note that, $\boldsymbol{\alpha}$ has nonzero entry in correspondence of target's AOA, therefore it can be seen as a sparse vector that can be evaluated using the SLIM devised in [12]. Interestingly, the grid spacing $\Delta\theta$ allows to manage the trade-off between the angular and amplitude estimation accuracy. In fact, the estimation accuracy of $\boldsymbol{\alpha}$ increases as $\Delta\theta$ increases, but with a consequent reduction in the angular estimation accuracy [12], [22]. This motivates our choice of first set $\Delta\theta$ to a wide value to accurately estimating $\boldsymbol{\alpha}$ and then refining the estimation of θ_t by means of a parabolic interpolation.

III. SLIM ALGORITHM FOR DOA ESTIMATION

In this section the sparse recovery algorithm SLIM of [12] for recovering sparse signals in Gaussian interference is described. To this end, we first assume that the interference covariance matrix $\boldsymbol{M}$ is known and exploits the same sparsity promoting prior probability density function (pdf) of $\boldsymbol{\alpha}$ as in [12], the estimate of $\boldsymbol{\alpha}$ in the context of maximum a posteriori (MAP) can be stated as

$$\widehat{\boldsymbol{\alpha}} = \arg\min_{\boldsymbol{\alpha}} \left\{ \left\| \boldsymbol{M}^{-1/2} (\boldsymbol{r} - \boldsymbol{S}\boldsymbol{\alpha}) \right\|^2 + \sum_{m=1}^{N_a} \frac{2}{q} \left(|\alpha_m|^q - 1 \right) \right\}, \tag{3}$$

where q is a parameter aimed at controlling the sparsity of $\boldsymbol{\alpha}$.

It is now worth to recall that the interference covariance matrix $\boldsymbol{M}$ is unknown in practical contexts and needs to be substituted by a proper estimate, say $\hat{\boldsymbol{M}}$, obtained from training data, resorting to a-priori information, or exploiting shrinkage or diagonal loaded structures [23]–[27]. Therefore, following the lead of [12], the iterative solution of problem (3) is given by

$$\boldsymbol{\alpha}^{(i+1)} = \left[\boldsymbol{S}^\dagger \hat{\boldsymbol{M}}^{-1} \boldsymbol{S} + \left(\tilde{\boldsymbol{P}}^{(i)} \right)^{-1} \right]^{-1} \boldsymbol{S}^\dagger \hat{\boldsymbol{M}}^{-1} \boldsymbol{r}, \tag{4}$$

where

$$\tilde{\boldsymbol{P}}^{(i)} = \textbf{diag}\left(\left[|\alpha_1^{(i)}|^{2-q}, \ldots, |\alpha_{N_a}^{(i)}|^{2-q} \right] \right). \tag{5}$$

The iterative procedure (4) is initialized with the unconstrained maximum likelihood (ML) estimate [23] of the m-th entry of $\boldsymbol{\alpha}$

$$\alpha_m^{(0)} = \frac{\boldsymbol{s}^\dagger(\theta_m) \hat{\boldsymbol{M}}^{-1} \boldsymbol{r}}{\boldsymbol{s}^\dagger(\theta_m) \hat{\boldsymbol{M}}^{-1} \boldsymbol{s}(\theta_m)}, \; m = 1, \cdots, N_a. \tag{6}$$

Finally, the parameter q is automatically selected exploiting the Bayesian information criterion (BIC) as in [12], [17].

IV. DOA REFINEMENT BASED ON PARABOLIC INTERPOLATION

This section describes the proposed refinement procedure of the estimated DOA of a sparse signal recovered with the SLIM given in Section III. The starting point is the estimated amplitude vector $\boldsymbol{\alpha}$ together with the corresponding angle locations, that are the points on the considered search grid spaced by $\Delta\theta$. Since the target DOA is the angle associated with the maximum of the modulus of $\boldsymbol{\alpha}$ values, it can be refined properly interpolating the values in $\boldsymbol{\alpha}$ contained. More precisely, the interpolation is performed on three points of the available vector, viz., the maximum and its two adjacent values. Figure 1 depicts an example of the magnitude of the $\boldsymbol{\alpha}$ values of a target as a function of the corresponding angles θ together with the representation of the real-valued parabolic interpolation.

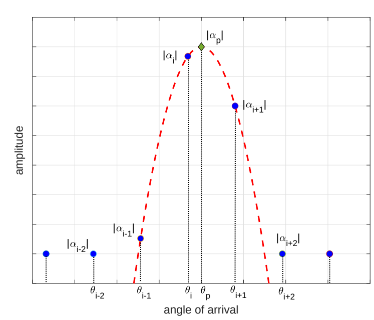

Figure 1. Magnitude of the $\boldsymbol{\alpha}$ values of a target with the real-valued parabolic interpolation.

A. Real-valued parabolic interpolation

The simplest case considers as interpolating function the real-valued parabola whose peak position is located at

$$\theta_p = \theta_i + \Delta\theta\delta_R \tag{7}$$

with

$$\delta_R = \frac{|\alpha_{i+1}| - |\alpha_{i-1}|}{4|\alpha_i| - 2|\alpha_{i+1}| - 2|\alpha_{i-1}|}. \tag{8}$$

B. Least Squares complex-valued parabolic interpolation

Herein, the interpolating function is a complex-valued parabola given by

$$\alpha = a\theta^2 + b\theta + c \tag{9}$$

with $\alpha, a, b, c \in \mathbb{C}$ and $\theta \in \mathbb{R}$. It is should be now underlined that, even if the meaning of peak is naturally defined in the real domain, it could be generalized abstracting this concept to the complex field. Therefore, similarly to the real-valued case, the peak position can be found solving a LS problem, whose solution is given by

$$\theta_p = \theta_i + \Delta\theta\delta_{LS} \tag{10}$$

with

$$\delta_{LS} = \Re\left\{\frac{\alpha_{i+1} - \alpha_{i-1}}{4\alpha_i - 2\alpha_{i+1} - 2\alpha_{i-1}}\right\}. \tag{11}$$

The proof for finding this solution is given in Appendix A.

C. Complex-valued parabolic interpolation by Jacobsen

This case refers also to a complex-valued interpolating parabola whose solution has been provided by Jacobsen in [28], [29] for accurate frequency estimating of a tone affected by noise by means of the Discrete Fourier Transform (DFT). Again, the peak position can be found by the following relation

$$\theta_p = \theta_i + \Delta\theta\delta_J \tag{12}$$

with

$$\delta_J = \Re\left\{\frac{\alpha_{i+1} - \alpha_{i-1}}{2\alpha_i - \alpha_{i+1} - \alpha_{i-1}}\right\}. \tag{13}$$

V. Performance analyses

This section is devoted at analyzing the performance of the proposed procedure aimed at providing a fine estimate of the DOA of a sparse recovered signal. To this end, the considered performance metric is the root mean square error (RMSE) of the estimated angle, that, due to the lack of a closed-form expression, is estimated through $M_c = 10^3$ independent Monte Carlo experiments, that is

$$\text{RMSE} = \sqrt{\frac{1}{M_c}\sum_{i=1}^{M_c}\left|\hat{\theta}_i - \theta_t\right|^2}, \tag{14}$$

where $\hat{\theta}_i$ is the AOA estimate at the i-th trial and θ_t is the actual target DOA modeled as $\theta_t \sim \mathcal{U}\,[5.4°, 5.6°]$. Simulations are conducted with reference to a radar system comprising $N = 8$ elements. Moreover, the interference scenario shares a Gaussian-shaped covariance, that is

$$\boldsymbol{M}(n,m) = \rho^{|n-m|^2}, \quad n, m = 1, \ldots, N, \tag{15}$$

with $\rho = 0.99$ the correlation coefficient of interference. Finally, the parameter q for the SLIM is discretized over a grid equal to $\{0.01, 0.1, 0.2, \ldots, 1\}$, whereas the SLIM itself is stopped after $N_{iter} = 25$ iterations.

The first case study considers the nominal pointing direction of the array at $0°$. In addition, the considered dictionary includes approximately the 3 dB beamwidth of the antenna beampattern, viz. $[-8°, 8°]$, with a discretization grid comprising $N_a = 9$ points equally spaced by $\Delta\theta = 2°$, as depicted in Figure 2(a). Analogously, the second case study herein analyzed shares the same parameter settings as the first, except for the discretization grid composed by $N_a = 17$ points equally separated by $\Delta\theta = 1°$, as in Figure 2(b).

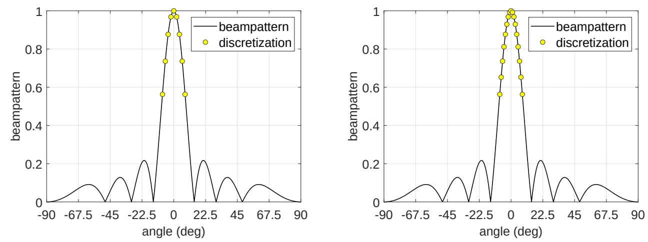

(a) (b)

Figure 2. Beampattern discretization with a) $N_a = 9$ ($\Delta\theta = 2°$) and b) $N_a = 17$ ($\Delta\theta = 1°$).

Fig. 3 plots the RMSE of the estimated angle computed through (14) versus signal to interference plus noise ratio (SINR) defined as

$$\text{SINR} = |\alpha|^2 \boldsymbol{s}^\dagger \boldsymbol{M}^{-1} \boldsymbol{s}. \tag{16}$$

The curves are related to the proposed method that is the LS complex-valued parabolic interpolation (called LS-SLIM), also in comparison with the complex-valued parabolic interpolation by Jacobsen (briefly indicated with J-SLIM), the real-valued parabola (referred to as R-SLIM), and the standard SLIM. Moreover, the deterministic CRLB for a ULA with a target embedded in colored interference is also plotted as performance benchmark [30], [31]. As the curves show, all the interpolating methods are capable of ensuring satisfactory performance improving the quality obtained by the SLIM. However, the LS-SLIM gives the best results together with the R-SLIM overcoming the J-SLIM for high SINR values. Moreover, as expected the evidence is that the all refinements suffer the poor SLIM estimates under low SINR regimes.

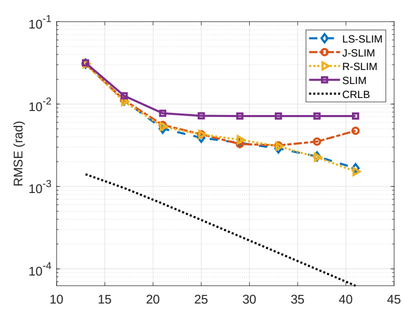

Figure 3. RMSE of the estimated angle for $N_a = 9$ ($\Delta\theta = 2°$) and $\theta_t \sim \mathcal{U}\,[5.4°, 5.6°]$.

To corroborate further the results shown in Fig. 3, in Fig. 4, the boxplots of the estimated angles are reported for different SINR values and setting $\theta_t = 5.5°$. Moreover, subplots refer to a) LS-SLIM, b) J-SLIM, c) R-SLIM, and d) SLIM. As before the boxplots demonstrate the effectiveness of the proposed approach in refining the DOA estimates provided by the SLIM. In fact, while the SLIM tends to polarize its estimation on the value $6°$ as the SINR increases (since this value lies on the discretization grid), the medians of the others are mostly correctly placed on the true value $\theta_t = 5.5°$ (with the LS showing the lowest dispersion of values) indicated with the black star ($\star$) in the figures.

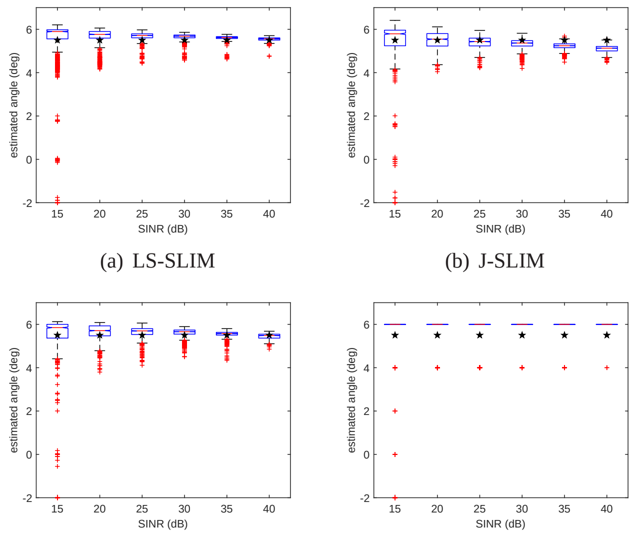

(a) LS-SLIM (b) J-SLIM

(c) R-SLIM (d) SLIM

Figure 4. Boxplot versus SINR for $N_a = 9$ ($\Delta\theta = 2°$) and $\theta_t = 5.5°$. Subplots refer to a) LS-SLIM, b) J-SLIM, c) R-SLIM, and d) SLIM.

The second case study considers the same scenario as before but with a denser grid for the computation of the SLIM with $N_a = 17$ points as depicted in Fig. 2(b). The result of this analysis is displayed in Fig. 3 as the RMSE of the estimated angle vs SINR. Again, from the curves behavior it can be recognized the effectiveness of the proposed approach in terms of DOA estimation refinement, observing almost the same trend of the curves. In fact, it is also worth to observe that these results do not significantly differ from those of the first study case. This can be justified by means of the following considerations. In fact, the SLIM is capable of accurately estimating $\boldsymbol{\alpha}$ using wide values of $\Delta\theta$, even if with a low accurate AOA. Then, the AOA estimation accuracy is improved applying the parabolic interpolation (as shown in the first test). It is tantamount to observe that, the AOA estimation accuracy can be also improved by reducing the grid step size of the SLIM. However, this improvement is paid in terms of accuracy loss in $\boldsymbol{\alpha}$ estimate as well as in a growth of the computational complexity of the SLIM that is essentially ruled by $\mathcal{O}(NN_a)$ (this is the situation analyzed in the second study case). By the way, these considerations motivate the use of the proposed procedure in practical implementations.

VI. Conclusion

In this letter, a two-stage procedure aimed at estimating the AOA of a radar target has been devised. Precisely, the first stage, exploiting the characteristics of the involved signals, resorts to a sparse recovery methodology to obtain a first

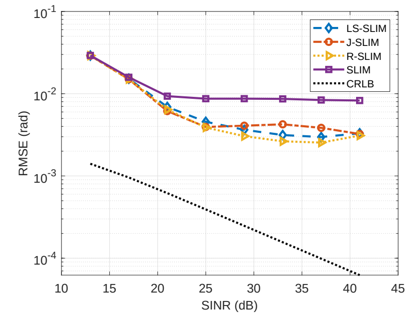

Figure 5. RMSE of the estimated angle for $N_a = 17$ ($\Delta\theta = 1°$) and $\theta_t \sim \mathcal{U}\,[5.4°, 5.6°]$.

estimate of the target's amplitude and AOA. At the next stage, the estimated AOA is refined using a complex-valued parabolic interpolation exploring the complex amplitude estimates given at the previous step. The grand advantage of the proposed method is the low computational cost due to the fact that it is possible to use a wide azimuth grid at the first sparse recovery stage, whose accuracy is then improved with the closed-form interpolation. Tests on numerical data have emphasized the effectiveness of the proposed approach in properly refining the AOA. Possible future works might extend the proposed framework to 2D (azimuth-elevation) estimation problems as well as to perform tests on measured data.

Acknowledgments

The authors thank Ms Cristiani Sara for carried-out part of simulations during her MSc thesis at University of Roma Tre.

Appendix

A. *Derivation of the solution* (11) *though LS*

The peak position of the complex parabola of (9) is obtained setting to zero its first derivative with respect to θ, that is

$$\frac{\partial \alpha}{\partial \theta} = 0 \quad \rightarrow \quad 2a\theta + b = 0 \tag{17}$$

that, since a and b are complex quantities, (17) can be cast in the following form

$$\begin{cases} 2\Re\{a\}\theta + \Re\{b\} = 0 \\ 2\Im\{a\}\theta + \Im\{b\} = 0 \end{cases}, \tag{18}$$

that in a more compact matrix form can be written as

$$2\begin{bmatrix} \Re\{a\} \\ \Im\{a\} \end{bmatrix}\theta = -\begin{bmatrix} \Re\{b\} \\ \Im\{b\} \end{bmatrix} \quad \rightarrow \quad 2\boldsymbol{a}\theta = -\boldsymbol{b}. \tag{19}$$

Equation (19) can be formalized as the following LS problem

$$\hat{\theta} = \arg\min_{\theta} \|2\boldsymbol{a}\theta + \boldsymbol{b}\|^2, \tag{20}$$

whose solution is given by

$$\begin{aligned} \hat{\theta} &= -\frac{1}{2}\left(\boldsymbol{a}^T\boldsymbol{a}\right)^{-1}\boldsymbol{a}^T\boldsymbol{b} = -\frac{1}{2}\frac{\|\boldsymbol{a}\|\|\boldsymbol{b}\|\cos(\phi_b - \phi_a)}{\|\boldsymbol{a}\|^2} \\ &= -\frac{1}{2}\frac{\|\boldsymbol{b}\|}{\|\boldsymbol{a}\|}\Re\left\{e^{j(\phi_b - \phi_a)}\right\} = \Re\left\{-\frac{b}{2a}\right\}, \end{aligned} \tag{21}$$

having indicated with ϕ_a and ϕ_b the phase of $\boldsymbol{a}$ and $\boldsymbol{b}$, respectively.

REFERENCES

[1] J. Capon, "High-Resolution Frequency-Wavenumber Spectrum Analysis," *Proceedings of the IEEE*, vol. 57, no. 8, pp. 1408–1418, 1969.

[2] R. Roy and T. Kailath, "ESPRIT-Estimation of Signal Parameters via Rotational Invariance Techniques," *IEEE Transactions on Acoustics, Speech, and Signal Processing*, vol. 37, no. 7, pp. 984–995, 1989.

[3] P. Stoica and K. C. Sharman, "Maximum Likelihood Methods for Direction-Of-Arrival Estimation," *IEEE Transactions on Acoustics, Speech, and Signal Processing*, vol. 38, no. 7, pp. 1132–1143, 1990.

[4] A. Farina, "Antenna-Based Signal Processing Techniques for Radar Systems," *Norwood, MA: Artech House*, 1992.

[5] P. Stoica and A. B. Gershman, "Maximum-Likelihood DOA Estimation by Data-Supported Grid Search," *IEEE Signal Processing Letters*, vol. 6, no. 10, pp. 273–275, 1999.

[6] M. Greco, F. Gini, A. Farina, and M. Rangaswamy, "DOA Estimation and Multi-User Interference in a Two-Radar System," *Signal processing*, vol. 89, no. 4, pp. 355–364, 2009.

[7] M. M. Hyder and K. Mahata, "Direction-of-Arrival Estimation Using a Mixed$\ell_{2,0}$Norm Approximation," *IEEE Transactions on Signal Processing*, vol. 58, no. 9, pp. 4646–4655, Sep. 2010.

[8] Z. Tan, Y. C. Eldar, and A. Nehorai, "Direction of Arrival Estimation Using Co-Prime Arrays: A Super Resolution Viewpoint," *IEEE Transactions on Signal Processing*, vol. 62, no. 21, pp. 5565–5576, Nov 2014.

[9] D. Ciuonzo, G. Romano, and R. Solimene, "Performance Analysis of Time-Reversal MUSIC," *IEEE Transactions on Signal Processing*, vol. 63, no. 10, pp. 2650–2662, 2015.

[10] Y. Chen, A. H. C. Ko, W. S. Tam, C. W. Kok, and H. C. So, "Non-Iterative DOA Estimation Using Discrete Fourier Transform Interpolation," *IEEE Access*, vol. 7, pp. 55 620–55 630, 2019.

[11] L. Chen, W. Qi, P. Liu, E. Yuan, Y. Zhao, and G. Ding, "Low-Complexity Joint 2-D DOA and TOA Estimation for Multipath OFDM Signals," *IEEE Signal Processing Letters*, vol. 26, no. 11, pp. 1583–1587, 2019.

[12] X. Tan, W. Roberts, J. Li, and P. Stoica, "Sparse Learning via Iterative Minimization With Application to MIMO Radar Imaging," *IEEE Transactions on Signal Processing*, vol. 59, no. 3, pp. 1088–1101, 2011.

[13] Z. Liu, Z. Huang, and Y. Zhou, "An Efficient Maximum Likelihood Method for Direction-of-Arrival Estimation via Sparse Bayesian Learning," *IEEE Transactions on Wireless Communications*, vol. 11, no. 10, pp. 1–11, October 2012.

[14] M. Carlin, P. Rocca, G. Oliveri, F. Viani, and A. Massa, "Directions-of-Arrival Estimation Through Bayesian Compressive Sensing Strategies," *IEEE Transactions on Antennas and Propagation*, vol. 61, no. 7, pp. 3828–3838, July 2013.

[15] Z. Yang, L. Xie, and C. Zhang, "Off-Grid Direction of Arrival Estimation Using Sparse Bayesian Inference," *IEEE Transactions on Signal Processing*, vol. 61, no. 1, pp. 38–43, Jan 2013.

[16] M. Ibrahim, F. Römer, R. Alieiev, G. Del Galdo, and R. S. Thomä, "On the Estimation of Grid Offsets in CS-based Direction-Of-Arrival Estimation," in *International Conference on Acoustics, Speech and Signal Processing (ICASSP)*. IEEE, 2014, pp. 6776–6780.

[17] S. Han, L. Pallotta, X. Huang, G. Giunta, and D. Orlando, "A Sparse Learning Approach to the Design of Radar Tunable Architectures with Enhanced Selectivity Properties," *IEEE Transactions on Aerospace and Electronic Systems*, vol. 56, no. 5, pp. 3840–3853, October 2020.

[18] E. Mosca, "Angle Estimation in Amplitude Comparison Monopulse Systems," *IEEE Transactions on Aerospace and Electronic Systems*, no. 2, pp. 205–212, 1969.

[19] A. Farina, G. Gabatel, and R. Sanzullo, "Estimation of Target Direction by Pseudo-Monopulse Algorithm," *Signal Processing*, vol. 80, no. 2, pp. 295–310, 2000.

[20] A. Farina, F. Gini, and M. Greco, "DOA Estimation by Exploiting the Amplitude Modulation induced by Antenna Scanning," *IEEE Transactions on Aerospace and Electronic Systems*, vol. 38, no. 4, pp. 1276–1286, 2002.

[21] M. Valeri, S. Barbarossa, A. Farina, and L. Timmoneri, "Monopulse Estimation of Target DOA in External Noise Fields with Adaptive Arrays," in *Proceedings of International Symposium on Phased Array Systems and Technology*. IEEE, 1996, pp. 386–390.

[22] D. Needell and J. Tropp, "CoSaMP: Iterative Signal Recovery from Incomplete and Inaccurate Samples," *Applied and Computational Harmonic Analysis*, vol. 26, no. 3, pp. 301–321, 2009.

[23] E. J. Kelly, "An Adaptive Detection Algorithm," *IEEE Transactions on Aerospace and Electronic Systems*, no. 2, pp. 115–127, 1986.

[24] F. C. Robey, D. R. Fuhrmann, E. J. Kelly, and R. Nitzberg, "A CFAR Adaptive Matched Filter Detector," *IEEE Transactions on Aerospace and Electronic Systems*, vol. 28, no. 1, pp. 208–216, 1992.

[25] A. Aubry, A. De Maio, L. Pallotta, and A. Farina, "Covariance Matrix Estimation via Geometric Barycenters and its Application to Radar Training Data Selection," *IET Radar, Sonar & Navigation*, vol. 7, no. 6, pp. 600–614, 2013.

[26] A. Aubry, A. De Maio, and L. Pallotta, "A Geometric Approach to Covariance Matrix Estimation and its Applications to Radar Problems," *IEEE Transactions on Signal Processing*, vol. 66, no. 4, pp. 907–922, 2018.

[27] A. De Maio, L. Pallotta, J. Li, and P. Stoica, "Loading Factor Estimation Under Affine Constraints on the Covariance Eigenvalues With Application to Radar Target Detection," *IEEE Transactions on Aerospace and Electronic Systems*, vol. 55, no. 3, pp. 1269–1283, 2019.

[28] E. Jacobsen, "On Local Interpolation of DFT Outputs," *Available online: http://www.ericjacobsen.org/FTinterp.pdf.[Accessed January 2013]*, 1994.

[29] E. Jacobsen and P. Kootsookos, "Fast, Accurate Frequency Estimators [DSP Tips & Tricks]," *IEEE Signal Processing Magazine*, vol. 24, no. 3, pp. 123–125, 2007.

[30] P. Stoica and A. Nehorai, "Performance Study of Conditional and Unconditional Direction-Of-Arrival Estimation," *IEEE Transactions on Acoustics, Speech, and Signal Processing*, vol. 38, no. 10, pp. 1783–1795, 1990.

[31] Y. Liang, W. Liu, Q. Shen, W. Cui, and S. Wu, "A Review of Closed-Form Cramér-Rao Bounds for DOA Estimation in the Presence of Gaussian Noise Under a Unified Framework," *IEEE Access*, vol. 8, pp. 175 101–175 124, 2020.